

Simulating Phase-Change Phenomena Using Gradient Augmented Level Set Approach

C. R. Lakshman Anumolu, Mridul Aanjaneya, Sifakis Eftychios, and Mario F. Trujillo *
Department of Mechanical Engineering
University of Wisconsin-Madison
Madison, WI 53706-1572 USA

Abstract

A sharp interface capturing approach is presented for two-phase flow simulations with phase change. The Gradient Augmented Level Set (GALS) method is coupled with the two-phase momentum and energy conservation equations to advect the liquid-gas interface and predict heat transfer with phase change. The Ghost Fluid Method (GFM) is adopted to discretize the advection and diffusion terms for velocity in computational cells located in the interfacial region. Furthermore, the GFM is also employed to treat the discontinuity in the stress tensor, velocity, and temperature gradient across the interface yielding a more accurate treatment in handling interfacial jump conditions. Thermal convection and diffusion terms are approximated by explicitly identifying the interface location, resulting in a sharp treatment for the energy solution. This sharp treatment is extended in estimating the interfacial mass transfer rate. At the computational cell, an n-cubic Hermite interpolation scheme is employed to describe the interface location, which is locally fourth-order accurate. This extent of subgrid level description provides an accurate methodology for treating the various interfacial processes with a high degree of sharpness. The ability to predict the interface and temperature evolutions accurately is illustrated by comparing numerical results with existing 1D to 3D analytical solutions.

*Corresponding author: mtrujillo@wisc.edu

Introduction

Heat transfer due to phase-change phenomena has wide industrial applications, such as cooling systems in nuclear reactors, refrigeration system, boilers, etc. Simulating such processes using computational resources provides the flexibility to predict thermo-dynamic quantities at any physical location, providing the framework for an in-depth analysis.

Simulating two-phase flows with phase-change using Computational Fluid Dynamics (CFD) techniques was pioneered by Welch [1], by explicitly tracking the interface using a moving triangular mesh. The earliest contributions towards simulating phase-change problems with topological changes are attributed to the works of Son and Dhir [2] and Juric and Tryggvason [3]. Son and Dhir [2] used the Level set (LS) [4] method to capture the liquid-vapor interface to simulate film boiling phenomena; though, it should be noted that the surface forces were treated by assuming a smeared interface. Alternatively, Juric and Tryggvason [3] developed a phase-change model using the Front Tracking (FT) [5] method. The results shown in [3] deal with high density ratios in 2D and are able to demonstrate film boiling.

Predicting phase-change phenomena using LS methods was originally introduced in [2] to simulate film boiling near critical pressures. Sharp interface treatment utilizing the Ghost Fluid Method (GFM) for modelling phase-change was introduced by Tanguy et al. [14] and Gibou et al. [15]. Numerical algorithms developed for phase change simulations in the context of LS have two things in common. First, the two-phase momentum and energy solutions are coupled with the classical LS approach to capture the interface. Second, a PDE based extrapolation technique [16] has been applied to enable smooth treatment of differential terms in the energy solution.

In the current work, the problem of heat transfer with phase change for two-phase system in the context of LS is revisited with the following new contributions:

1. The interface is identified within each computational cell by a tensor product of cubic Hermite basis polynomials rendering fourth-order spatial accuracy locally. This provides a more accurate framework for the implementation of the Ghost Fluid Method (GFM) in the discretization of the diffusion and convection terms of the momentum equation, as well as the treatment of the associated jump conditions.
2. Sharp treatment for the thermal convection and diffusion terms is employed by explicitly locating the interface with the aid of the cubic-Hermite polynomials.
3. Rather, than transporting the interface (\mathbf{x}_I) using the liquid velocity alone [14] or vapor velocity alone [18] in conjunction with mass

jump conditions, the interface in the present work is advected utilizing the liquid velocity in liquid phase region and the vapor velocity in vapor phase region, again in conjunction with the solution of mass jump conditions.

4. High order accurate reinitialization strategy [19] is employed to redistance the level set function and its gradient.

The current numerical approach is verified by considering a range of test cases from 1D to 3D by using known analytical solutions. In the following sections, an overview of the numerical method followed by test results are presented.

Numerical Method

The proposed numerical method utilizes a staggered grid arrangement, where the fluid velocities are stored on cell faces and all other variables are stored at cell-centers (level set field and its gradient, pressure, temperature and thermo-physical properties).

At the start of the simulation, the following variables are given; level set (ϕ), its gradient ($\nabla\phi$), fluid velocities i.e. liquid velocity (\mathbf{u}^L) and vapor velocity (\mathbf{u}^V), temperature (T), and the thermo-physical properties of fluids, such as density (ρ), dynamic viscosity (μ), thermal conductivity (k), and specific heat capacity (c_p). Using these flow variables, a step-by-step overview of the numerical approach is described below.

Algorithm

1. Compute temperature gradients at interfacial cells by enforcing Dirichlet boundary condition at the interface for temperature, using second order accurate non-uniform stencils.
2. Extrapolate temperature gradients from liquid phase to vapor phase and vice-versa. This ensures that, liquid temperature gradients and vapor temperature gradients are available at all interfacial cells irrespective of the fluid phase present at a given cell. In the present work normal-wise constant extrapolation [16] is employed to extrapolate each gradient component.
3. Extrapolate interfacial mass transfer rate from interfacial cells that belong to the liquid phase to all cells that contain liquid. Repeat the same procedure for cells occupying the vapor region. Similar to the above step, a normal-wise constant extrapolation [16] is employed.
4. Compute mass transfer rate (\dot{m}) at all cell faces using linear interpolation.
5. Compute ghost values for the liquid velocity in vapor region using the velocity jump condition. Repeat the similar computation to populate ghost values for the vapor velocity.
6. Compute fluid velocities at all centers using linear interpolation.

7. Compute the level set velocity using the available fluid velocities and mass transfer rates at all cell centers.
8. Advect the level set field and its gradient using Gradient Augmented Level Set (GALS) [20] approach.
9. Reinitialize the level set and its gradient fields using Hermite-polynomial based reinitialization [19] method.
10. Solve the two-phase momentum equation in both liquid and vapor phases using Chorin's projection method [21]. Note that, while solving the governing equations in liquid phase, ghost values for velocity are used near the interfacial region, and similarly ghost values for vapor phase are used while solving the equations in vapor phase.
11. Solve the two-phase energy equation at all cell centers to update temperature of both phases. A sharp treatment is employed while computing the convection and diffusion terms, which helps in capturing the jump in material properties accurately near the interface.

Results

The proposed numerical method is verified on several test cases, ranging from 1D to 3D. Comparisons between analytical and numerical results for the temporal evolution of interface location and temperature are presented below.

1D Stefan Problem

The schematic of this test case is illustrated in Fig. 1, where vapor and liquid phases are shown separated by the phase-interface.

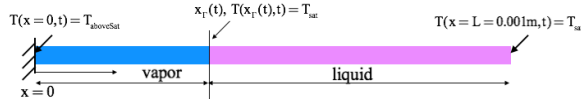


Figure 1. Layout for 1D Stefan problem.

The temperature field and interface location for the setup are initialized using the analytical solution at time $t=0.1s$ [6]. Comparisons between numerical and analytical results for interface locations at different time instances are shown in Fig. 2. Good agreement is observed between them even at the coarsest grid resolution. Figure 3 presents the temperature field comparison with the analytical solution at $t=0.3s$. Second order convergence is observed for the temperature field prediction, which is shown in Table 1.

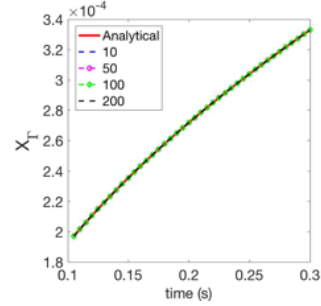


Figure 2. Interface location as a function of time.

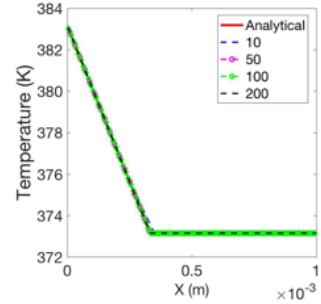


Figure 3. Fluid temperature at $t=0.3s$.

Grid	L_1 error (T)	Rate
10	1.51e-01	-
50	6.26e-03	1.98
100	1.65e-03	1.92
200	4.76e-04	1.79

Table 1. L_1 errors for fluid temperature at $t=0.3s$.

Vapor Bubble (2D & 3D) Growth Under Zero Gravity and With Prescribed \dot{m}

Vapor bubble growth is predicted in both 2D and 3D, given the interface mass transfer rate (\dot{m}). This test case highlights the numerical algorithm's ability to capture the velocity jump. The calculation of the bubble growth rate is used as a metric to demonstrate this.

Temporal evolution of the vapor bubble for different grid levels is presented in Fig. 4. Relative percentage deviation in the bubble radius from analytical solution is presented in Table 2. Results show first order convergence in predicting interface motion, this is due to the adoption of first order accurate GFM approach, which is currently being modified by including interface location with higher order accuracy. We would also like to note that, the percentage errors observed are about half the magnitude reported in [18].

This 2D vapor bubble case is extended to 3D, whose surface at three different time instances is shown in Fig. 5. The radius of the 3D bubble, as a function of time, is plotted in Fig. 6, which shows a good agreement with the analytical result.

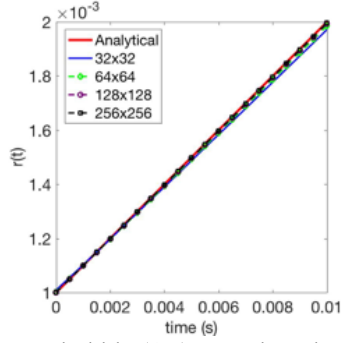


Figure 4. Vapor bubble (2D) growth under constant \dot{m} .

Grid	Relative error in $r(t)$ (%)	Rate
32x32	1.65	-
64x64	0.79	1.07
128x128	0.33	1.26
256x256	0.17	0.98

Table 2. Relative percentage error in bubble radius at $t=0.01$ s.

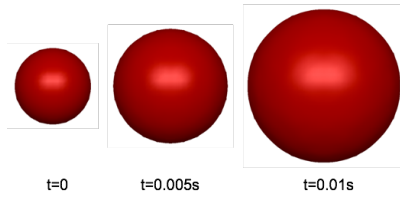


Figure 5. 3D visualization of vapor bubble growth under constant \dot{m} .

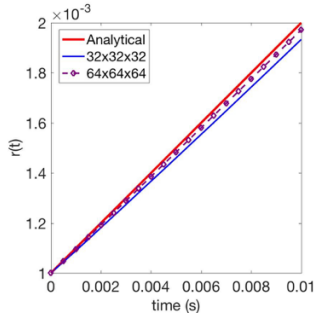


Figure 6. 3D Vapor bubble growth under constant \dot{m} .

Vapor Bubble (2D) Growth Immersed in Super-Saturated Liquid Under Zero Gravity Condition

Growth of a 2D vapor bubble immersed in a super heated liquid due to phase change is studied in this test case. The analytical solution for such a system was derived by Scriven [22], and is presented in [6, 18].

A vapor bubble of radius $r=5 \times 10^{-4}$ m is considered as the initial condition in a domain of $[0, 0.006] \times [0, 0.012]$ m. This setup corresponds to the radius of the bubble at $t_0=0.03729$ s, as per the analytical solution. Temperature in the computational domain is initialized with the analytical values at t_0 . Three grid

levels (64x128, 128x256 and 256x512) are considered for the numerical simulation, which is ran until $t=0.14916$ s ($= 4t_0$).

The computed temperature field in comparison with the analytical solution is shown in Fig. 7. It should be noted that the jump in temperature gradient is captured near the interface. Comparison of the vapor bubble radius between numerical and analytical results is presented in Fig. 8. Results show an accurate prediction of the temperature evolution and bubble growth using the presented numerical approach.

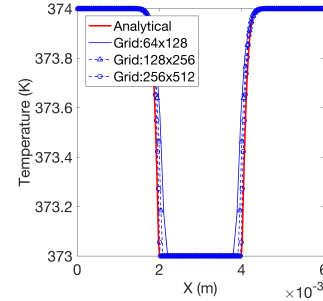


Figure 7. Radial temperature distribution of fluid along the center of vapor bubble at $t=0.14916$ s.

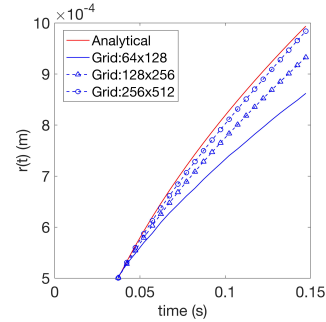


Figure 8. Growth of a 2D vapor bubble immersed in super heated liquid.

Conclusions

Test cases ranging from 1D to 3D are presented, and results show 2nd order convergence in predicting temperature field for the Stefan' problem. Employing high order advection and reinitialization methods in conjunction with implementing the correct velocity jump conditions to compute interface velocities yielded superior results over the published works. This is demonstrated in the 2D bubble growth test case with prescribed mass transfer rate. Convergence was clearly noted in the results for a 2D bubble growth immersed in super-heated liquid test case. Further verification that include, parametric study on the growing bubble test case with different Jakob numbers, will be performed. This will provide a range of physical conditions, with varying degree of the sensible heat transfer, that the proposed numerical method can accurately simulate. The ability to simulate phase-change process under the

effects of gravity, simulation of the film boiling phenomena will be part of our future verification tests.

References

1. S.W.J. Welch; *Journal of Computational Physics*; 121 (1995) 142-154.
2. G. Son and V.K. Dhir; *Journal of Heat Transfer*; 120 (1998) 183-192.
3. D. Juric and G. Tryggvason; *International Journal of Multiphase Flow*; 24 (1998) 387-410.
4. S.J. Osher and R.P. Fedkiw; *Springer: New York NY 10010*, 2002.
5. G. Tryggvason, B. Bunner, A. Esmarelli, D. Juric, N. Al-Rawahi, W. Tauber, J. Han, S. Nas, and Y.-J. Jan; *Journal of Computational Physics*; 169 (2001) 708-759.
6. Y. Sato and B. Niceno; *Journal of Computational Physics*; 249 (2013) 127-161.
7. S.W.J. Welch and J. Wilson; *Journal of Computational Physics*; 160 (2000) 662-682.
8. D.L. Youngs; *K.W. Morton and M.J. Baines (eds); Numerical Methods for Fluid Dynamics, Academic, New York*, (1982) 273-285.
9. M. Rudman; *International Journal for Numerical Methods in Fluids*; 24 (1997) 671-691.
10. G. Son, V.K. Dhir, N. Ramanujapu; *Journal of Heat Transfer*; 121 (1999) 623-631.
11. G. Son, V.K. Dhir; *International Journal of Heat and Mass Transfer*; 51 (2008) 2566-2582.
12. G. Son, N. Ramanujapu, V.K. Dhir; *Journal of Heat Transfer*; 124 (2002) 51-62.
13. A. Mukherjee, V.K. Dhir; *Journal of Heat Transfer*; 126 (2004) 1023-1039.
14. S. Tanguy, T. Menard, A. Berlemont; *Journal of Computational Physics*; 221 (2007) 837-853.
15. F. Gibou, L. Chen, D. Nguyen, S. Banerjee; *Journal of Computational Physics*; 222 (2007) 536-555.
16. T.D. Aslam; *Journal of Computational Physics*; 193 (2004) 349-355.
17. G. Son, V.K. Dhir; *International Journal of Heat and Mass Transfer*; 51 (2008) 1156-1167.
18. S. Tanguy, M. Sagan, B. Lalanne, F. Couderc, C. Colin; *Journal of Computational Physics*; 264 (2014) 1-22.
19. L. Anumolu and M. F. Trujillo; *International Journal for Numerical Methods in Fluids*; 73 (2013) 1011-1041.
20. J.-C Nave, R.R. Rosales, B. Seibold; *Journal of Computational Physics*; 229 (2010) 3802-382
21. A. Chorin; *Journal of Computational Physics*; 2 (1967) 12-26.
22. E. Scriven; *Chem. Eng. Sci.*; 10 (19